Contents lists available at ScienceDirect

Chemical Engineering Research and Design

journal homepage: www.elsevier.com/locate/cherd

Coupled PermSMBR – Process design and development for 1,1-dibutoxyethane production☆

Carla S.M. Pereira, Viviana M.T.M. Silva, Alírio E. Rodrigues*

LSRE – Laboratory of Separation and Reaction Engineering – Associate Laboratory LSRE/LCM, Faculdade de Engenharia, Universidade do Porto, rua Dr. Roberto Frias, 4200-465 Porto, Portugal

A B S T R A C T

In this work, a new configuration of the simulated moving bed membrane reactor (PermSMBR) technology is presented, the coupled PermSMBR, where the tubular membranes are located after fixed-bed columns packed with the catalyst/adsorbent. By this way the membranes are not in contact with the solid, which from an industrial point of view is easier to implement since the process of membranes installation/replacement and clean-up is simpler than in the previous considered set-up (tubular membranes packed with the catalyst/adsorbent – integrated PermSMBR). The 1,1-dibutoxyethane production is used, as an example, and the features of the new "coupled PermSMBR" and the previous set-up (integrated PermSMBR) are discussed. The coupled PermSMBR revealed to be a very attractive solution for the sustainable 1,1-dibutoxyethane production, proved by the high productivity and low desorbent consumption obtained within the studied conditions.

Keywords: Process intensification; Membrane reactors; Simulated moving bed reactor; Hybrid technologies; 1,1-Dibutoxyethane; Silica membranes; Amberlyst-15

1. Introduction

The simulated moving bed membrane reactor (PermSMBR) is a recently developed technology that consists of the integration of permselective membranes with the simulated moving bed reactor (SMBR) (Silva et al., 2009). The SMBR is implemented in well-known, but nontrivial, SMB equipment (Broughton and Gerhold, 1961), where the columns are packed with a solid catalyst with adsorptive properties or with a mixture of solid catalyst and adsorbent particles. The standard SMBR configuration comprises two inlet streams (feed and desorbent) and two outlet streams (extract and raffinate) and the countercurrent solid movement is simulated by a synchronous shift of these streams by one column in the direction of the fluid, at regular time intervals called the switching time. If the feed comprises two reactants (A and B), in which, for instance A, is used as desorbent, and A and B react to give two products, C and D, the latter being more adsorbed than the former, then a mixture of D and A is obtained in the extract and a mixture of C and A in the raffinate.

The inlet/outlet streams divide the unit into four different sections, each one with a specific role (described in a previous work (Rodrigues et al., 2012)) and having a given number of columns (see Fig. 1). This is the SMBR principle of operation which is similar to the one of the PermSMBR. However, in the new equipment each column is replaced by a set of tubular membranes packed with the solid (catalyst with adsorptive properties) or the mixture of solids (catalyst and adsorbent) (Fig. 2). Besides, another stream is collected: the permeate stream that combines all the flows removed through the membrane; the permeate is therefore rich in the product for which the membranes are selective. Depending on the system, different membrane processes can be applied as microfiltration, ultrafiltration, vapour permeation, pervaporation, among others.

* *Corresponding author*. Tel.: +351 225081686; fax: +351 225081674.
E-mail address: cpereir@fe.up.pt (C.S.M. Pereira).

Received 9 April 2013; Received in revised form 24 September 2013; Accepted 16 November 2013
Available online 28 November 2013
0263-8762/$ – see front matter © 2013 The Authors. Published by Elsevier B.V. All rights reserved.
http://dx.doi.org/10.1016/j.cherd.2013.11.015

Nomenclature

a_i	liquid-phase activity of component i in bulk side
A_m	membrane area per unit reactor volume ($m^2_{membrane}/m^3_{bulk}$)
C	liquid phase concentration (mol/m^3)
$\bar{C}_p$	average liquid phase concentration inside the particle (mol/m^3)
D_{ax}	axial dispersion coefficient (m^2/min)
DC	desorbent consumption (m^3/mol)
d_{int}	membrane internal diameter (m)
J_i	permeate flux of species i (mol/(m^{2}min))
k_{bl}	boundary layer mass transfer coefficient (m/s)
k_e	external mass transfer coefficient (m/s)
k_i	internal mass transfer coefficient (m/s)
K_L	global mass transfer coefficient (m/s)
k_{ov}	global membrane mass transfer coefficient (mol/(m^2 s Pa))
L	column length (m)
L_m	membrane length (m)
n	total number of components
N_c	total number of columns
p_i^0	saturation pressure of component i (bar)
P_{perm}	total pressure on the permeate side (bar)
PR	raffinate productivity ($kg_C/(L_{resin}\ day)$)
PUR	raffinate purity (%)
PUX	extract purity (%)
q	solid phase concentration in equilibrium with the fluid concentration inside the particle (mol/L)
Q	volumetric flow rate (L/min)
Q_{memb}	permeance (mol min^{-1} m^{-2} Pa^{-1})
r	rate of reaction (mol kg^{-1} min^{-1})
Re	Reynolds number
Re_p	Reynolds number relative to particle
r_p	particle radius (m)
Sc	Schmidt number
Sh	Sherwood number
t	time variable (min)
$t*$	switching time (min)
u	interstitial velocity (m/min)
v	superficial velocity (m/min)
V_C	volume of packed column (m^3)
$V_{mol,i}$	molar volume of species i (L/mol)
X	acetaldehyde conversion
y_i	molar fraction in the vapour phase of component i
z	axial coordinate (m)

Greek letters

γ^*	activity coefficient
ε	bulk porosity
ε_p	particle porosity
υ_i	stoichiometric coefficient of component i
ρ_b	bulk density (kg/m^3)
ρ_p	particle density (kg/m^3)
μ	viscosity (cP)
η	effectiveness factor of the catalyst
ΔP	pressure drop (Pa)
Φ	sphericity of the particles

Subscripts

i	relative to component i (i = A, B, C, D)
j	relative to section (j = 1, 2, 3, 4)
k	relative to column in coupled PermSMBR
m	relative to membrane module in coupled PermSMBR
0	relative to initial conditions
A	relative to n-butanol
B	relative to acetaldehyde
C	relative to 1,1-dibutoxyethane
D	relative to water
F	relative to the feed
p	relative to the particle
R	relative to raffinate
Rec	relative to recycle
X	relative to extract

The PermSMBR concept was already evaluated for the production of acetals (1,1-diethoxyethane and 1,1-dibutoxyethane) and a green solvent (ethyl lactate), using Amberlyst-15 wet (A15) resin as catalyst/adsorbent and silica membranes (from Pervatech BV, the Netherlands) for water dehydration (by product in both acetalization and esterification reactions) (Silva et al., 2010; Pereira et al., 2012). The results showed a productivity enhancement accompanied by a significant reduction on the solvent consumption when compared with reactive distillation and/or the SMBR technology, proving this equipment high potential for the production of oxygenated compounds.

In this work, a new PermSMBR configuration is proposed, where each SMBR column is followed by a membrane module – the coupled PermSMBR (see Fig. 3). In the coupled PermSMBR the membranes will not be in contact with the catalyst/adsorbent, which from an industrial point of view will be easier to implement since the process of membranes installation/replacement and clean-up is simpler. Moreover, the mechanical and chemical resistances of membranes will not be compromised by the catalyst/adsorbent presence. The assessment of this new set-up is made using, as an example, the production of 1,1-dibutoxyethane (DBE) and comparing its performance with the one of the SMBR and integrated PermSMBR under different operating conditions.

DBE was selected since it can be produced from common bio-refinery building blocks (n-butanol and acetaldehyde) according to Scheme 1, and used as green fuel additive enhancing the renewable fraction in diesel, which positively contributes for the important European environmental commitment that aims to replace 10% of total transport fuels by biofuels by 2020 (UE Directive 2009/28/EC). Moreover, DBE diesel blends have higher cetane numbers than diesel (Boennhoff and Obenaus, 1980).

2. Mathematical model of the coupled PermSMBR

As for the previous studied PermSMBR configuration that will be called integrated PermSMBR, the mathematical model used

$$2\ \text{n-butanol} + \text{acetaldehyde} \xleftrightarrow{H^+} \text{DBE} + \text{Water}$$

Scheme 1

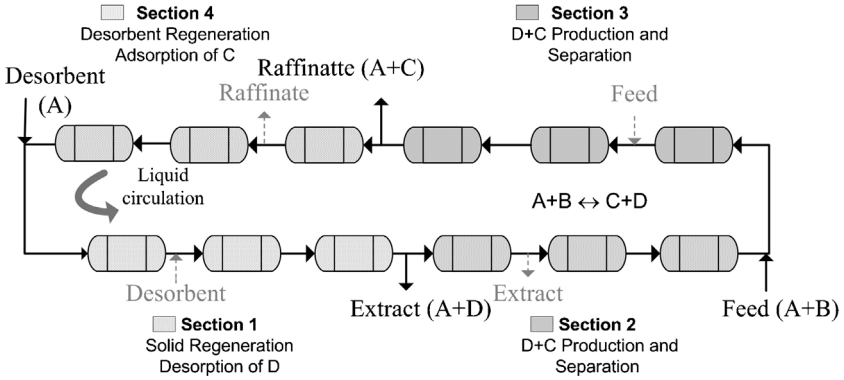

Fig. 1 – Schematic representation of a SMBR unit with 4 sections and 3 columns per section considering a reaction of type A + B ↔ C + D, where C is the less adsorbed product and D is the most adsorbed one. The dashed arrows represent the port switch.

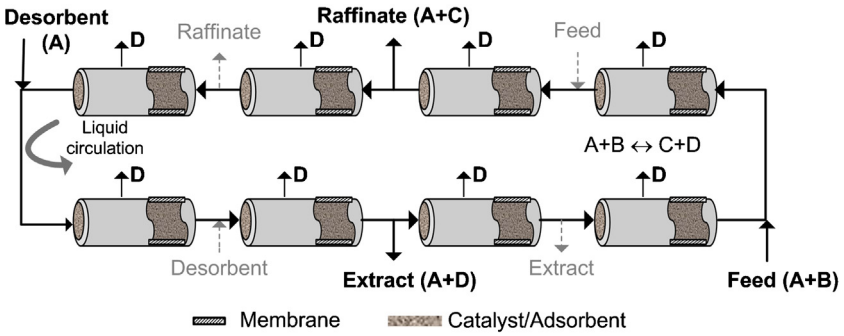

Fig. 2 – Schematic representation of an integrated PermSMBR unit with 4 sections and 2 columns per section considering a reaction of type A + B ↔ C + D, where C is the less adsorbed product and D is the most adsorbed product and the product for which the membrane is selective. The dashed arrows represent the port switch.

to describe the behaviour of the coupled PermSMBR considers axial dispersion flow for the bulk fluid phase, linear driving force (LDF) approximation for the inter and intra-particle mass transfer rates (lumped rate model), Langmuir–Hinshelwood rate model in terms of activities (Graça et al., 2010b), multi-component adsorption equilibrium at the adsorbent phase described by a Langmuir type isotherm (Graça et al., 2010a), constant porosity and length of the packed beds, membrane permeation described by the solution-diffusion model (Pereira et al., 2012), membrane concentration polarization, liquid velocity variations due to reaction, adsorption/desorption rates (in the packed beds) and due to species permeation (in the membrane modules), activity coefficients based on the UNIFAC model (Graça et al., 2010b) and isothermal operation.

A summary of the reaction kinetics, multi-component adsorption equilibrium isotherms and permeation performance, determined in previous works, is presented in Appendix A.

The model equations for the coupled PermSMBR are:

Bulk fluid mass balance to component i in column k

$$\frac{\partial C_{ik}}{\partial t} + \frac{\partial (C_{ik} u_k)}{\partial z} + \frac{(1-\varepsilon)}{\varepsilon} \frac{3}{r_p} k_{Lik} (C_{ik} - \overline{C}_{p,ik}) = D_{ax,k} \frac{\partial^2 C_{ik}}{\partial z^2} \quad (1)$$

where C_{ik} and $\bar{C}_{p,ik}$ are the bulk and average particle concentrations in the liquid phase of species i in column k, respectively; $k_{L,ik}$ is the global mass transfer coefficient of the component i; ε is the bulk porosity; t is the time variable; z is the axial coordinate; $D_{ax,k}$ is the axial dispersion coefficient in column

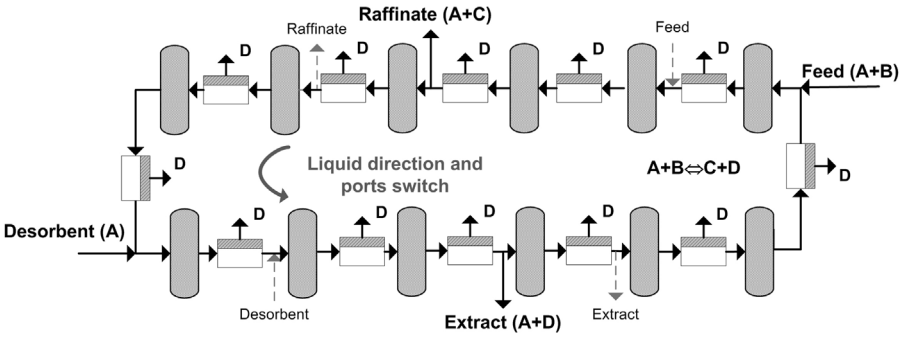

Fig. 3 – Schematic representation of a coupled PermSMBR unit with 4 sections and 3 columns plus 3 membrane modules per section considering a reaction of type A + B ↔ C + D, where C is the less adsorbed product and D is the most adsorbed product and also the product for which the membrane is selective. The dashed arrows represent the port switch.

k; u_k is the interstitial velocity in column k; r_p is the particle radius.

The global mass transfer coefficient (k_L), which combines the external (k_e) and internal (k_i) mass transfer coefficients for adsorbable species (Santacesaria et al., 1982) is defined, for each component, as:

$$\frac{1}{k_L} = \frac{1}{k_e} + \frac{1}{\varepsilon_p k_i} \tag{2}$$

where ε_p is the particle porosity. The external mass transfer coefficient was calculated as a function of the Reynolds number and the Schmidt number, using the Wilson and Geankoplis correlation (Ruthven, 1984), while the internal mass transfer coefficient was estimated by $k_i = 5D_m/(r_p\tau)$ (Glueckauf, 1955). The prediction of the species diffusivity (D_m) was made using the Perkins and Geankoplis method (Perkins and Geankoplis, 1969), and further details concerning its calculation can be found in Graça et al. (2010a) work. The axial dispersion coefficient (D_{ax}) determination is presented in detail in a previous work (Silva and Rodrigues, 2002).

Pellet mass balance to component i, in column k

$$\varepsilon_p \frac{\partial \overline{C}_{p,ik}}{\partial t} + (1-\varepsilon_p)\frac{\partial q_{ik}}{\partial t} = \frac{3}{r_p} k_{L,ik}(C_{ik} - \overline{C}_{p,ik}) + \upsilon_i \rho_p r(\overline{C}_{p,ik}) \tag{3}$$

where q_{ik} is the average adsorbed phase concentration of species i in column k in equilibrium with $\overline{C}_{p,ik}$, υ_i is the stoichiometric coefficient of component i, ρ_p the particle density and r is the chemical reaction rate relative to the average particle concentrations in the fluid phase.

Interstitial fluid velocity variation calculated from the total mass balance

$$\frac{du_k}{dz} = -\frac{(1-\varepsilon)}{\varepsilon}\frac{3}{r_p}\sum_{i=1}^{n} k_{L,ik} V_{mol,i}(C_{ik} - \overline{C}_{p,ik}) \tag{4}$$

where $V_{mol,i}$ is the molar volume of component i; and n is the total number of components.

Mass balance to component i in the retentate side of membrane m

$$\frac{\partial C_{im}}{\partial t} + \frac{\partial (C_{im}\upsilon_m)}{\partial z} + A_m J_{im} = D_{ax,m}\frac{\partial^2 C_{im}}{\partial z^2} \tag{5}$$

where A_m is the membrane area per volume; and J_{im} is the permeate flux of species i in the membrane m defined as:

$$J_i = k_{ov,i}(a_i p_i^0 - y_i P_{perm}) \tag{6}$$

where a_i is the activity of component i in bulk; p_i^0 is the saturation pressure of component i; P_{perm} is the total pressure on the permeate side; y_i is the molar fraction of component i in the vapour phase (permeate side), $y_i = J_i/\sum_{i=1}^{n} J_i$; and $k_{ov,i}$ is the global membrane mass transfer coefficient, which combines the resistance due to the diffusive transport in the boundary layer with the membrane resistance (Wijmans et al., 1996):

$$\frac{1}{k_{ov,i}} = \frac{1}{Q_{memb,i}} + \frac{\gamma_i^* p_i^0 V_{mol,i}}{k_{bl,i}} \tag{7}$$

in which $Q_{memb,i}$ is the permeance of component i through the membrane; γ_i^* is the activity coefficient of component i; and k_{bl} is the boundary layer mass transfer coefficient. For laminar flow and Graetz number ($d_{int}^2 u/(D_m L)$) much larger than one, the mass transfer coefficient for transport in the boundary layer, k_{bl}, is determined by the Lévêque correlation (Lévêque, 1928):

$$Sh = 1.62 Re^{0.33} Sc^{0.33}\left(\frac{d_{int}}{L_m}\right)^{0.33} \quad (Re < 2300) \tag{8}$$

where $Sh = k_{bl}d_{int}/D_m$ and $Re = \rho d_{int}\upsilon/\mu$ are the Sherwood and Reynolds numbers relative to membrane, respectively; $Sc = \mu/(\rho D_m)$ is the Schmidt number; d_{int} is the inside diameter of the membrane; L_m is the membrane length; ρ and μ are the bulk liquid mixture density and viscosity, respectively.

The axial dispersion coefficient in the retentate side of the membrane ($D_{ax,m}$) was estimated using the following expression (Levenspiel, 1999):

$$\frac{D_{ax,m}}{\upsilon L_m} = \frac{1}{Re \cdot Sc} + \frac{Re \cdot Sc}{192} \tag{9}$$

Fluid velocity variation in membrane m

$$\frac{d\upsilon_m}{dz} = -A_m \sum_{i=1}^{n} J_{im} V_{mol,i} \tag{10}$$

Mass balances at the nodes of the inlet and outlet lines:

$$\text{Desorbent node } (j=1): \quad C_{i(j=4)}|_{z=L_4} = \frac{Q_1|_{z=0}}{Q_4|_{z=L_4}} C_{i(j=1)}|_{z=0} - \frac{Q_D}{Q_4|_{z=L_4}} C_i^D \tag{11}$$

$$\text{Extract } (j=2) \text{ and raffinate } (j=4) \text{ and columns nodes}: \quad C_{i(j-1)}|_{z=L_{(j-1)}} = C_{i(j)}|_{z=0} \tag{12}$$

$$\text{Feed node } (j=3): \quad C_{i(j=2)}|_{z=L_2} = \frac{Q_3|_{z=0}}{Q_2|_{z=L_2}} C_{i(j=3)}|_{z=0} - \frac{Q_F}{Q_2|_{z=L_2}} C_i^F \tag{13}$$

where j is relative to section of the PermSMBR unit ($j = 1, 2, 3, 4$) and

- $Q_1|_{z=0} = Q_4|_{z=L_4} + Q_{Ds}$ Desorbent (D) node; (14)
- $Q_2|_{z=0} = Q_1|_{z=L_1} - Q_X$ Extract (X) node; (15)
- $Q_3|_{z=0} = Q_2|_{z=L_2} + Q_F$ Feed (F) node; (16)
- $Q_4|_{z=0} = Q_3|_{z=L_3} - Q_R$ Raffinate (R) node; (17)

For the remaining columns:

- $Q_k|_{z=L_k} = Q_m|_{z=0}$ (18)
- $Q_m|_{z=L_m} = Q_{k+1}|_{z=0}$ (19)

Initial and Danckwerts boundary conditions:

$$t = 0: \quad C_{im} = C_{ik} = \bar{C}_{p,ik} = C_{ik,0} \text{ and } q_{ik} = q_{ik,0} \tag{20}$$

$$z = 0: \quad u_k C_{ik}|_{z=0} - D_{ax,k}\left.\frac{\partial C_{ik}}{\partial z}\right|_{z=0} = u_k C_{ik,F} \tag{21}$$

$$v_m C_{im}|_{z=0} - D_{ax,m} \left.\frac{\partial C_{im}}{\partial z}\right|_{z=0} = v_m C_{ik}|_{z=L} \quad (22)$$

$$z = L: \quad \left.\frac{\partial C_{ik}}{\partial z}\right|_{z=L_k} = 0 \quad (23)$$

$$\left.\frac{\partial C_{im}}{\partial z}\right|_{z=L_m} = 0 \quad (24)$$

where the subscripts F and 0 refer to the feed and initial states, respectively.

3. Performance parameters

The PermSMBR unit performance parameters are: extract and raffinate purity, conversion, productivity and desorbent consumption. The definitions of the purity in free desorbent basis and the unit productivity in terms of DBE produced and collected in the raffinate per amount of adsorbent/catalyst, obtained by the PermSMBR model at the cyclic steady state over a complete cycle, are presented in Table 1.

4. Numerical solution

The model equations were solved numerically by using the gPROMS-general PROcess Modelling System version: 3.5.3. The mathematical model involves a system of partial and algebraic equations (PDAEs). The axial domain was discretized using second order orthogonal collocation in finite elements method (OCFEM) over twenty finite elements. The system of ordinary differential and algebraic equations (ODAEs) was integrated over time using the DASOLV integrator implementation in gPROMS. For all simulations was set a tolerance value equal to 10^{-5}.

5. Results and discussion

5.1. Geometrical specifications

The SMBR geometrical specifications are the ones of an SMB unit available in our laboratory and used, in a previous work, for technology demonstration for DBE production (Graça et al., 2011): the Licosep 12-26 SMB Pilot Unit (Novasep, France) with 12 Superformance SP 230 × 26 (length × ID, mm) columns packed with the commercial ion-exchange resin A15. The PermSMBR geometrical specifications considered are 12 columns, where each column has 13 commercial hydrophilic tubular membranes (Pervatech BV) (25.45 cm length and 0.7 cm diameter) packed with the resin A15 (inside the membrane tube). The length and the number of membranes were set by imposing the same mass of catalyst and effective cross-sectional area than that of the SMBR unit.

The coupled PermSMBR consists in 12 fixed-bed columns, where each column is followed by a membrane module comprising 13 parallel hydrophilic tubular membranes (Pervatech BV). The geometry and number of the fixed-bed columns and the geometry and number of the membranes were set in order to have the same amount of catalyst/adsorbent and the same membrane area than in the PermSMBR, respectively.

A summary of the characteristics of the columns for each one of the technologies is presented in Table 2.

5.2. SMBR, integrated PermSMBR and coupled PermSMBR technologies

5.2.1. Reactive separation regions

The SMBR and the integrated PermSMBR performances were already evaluated and compared for the synthesis of 1,1-dibutoxyethane (DBE), through their reactive separation regions (Pereira et al., 2012), which are feasible regions that define the operating conditions in sections 2 and 3, for pre-set conditions in sections 1 and 4, in order to obtain specific purity (for both extract and raffinate streams) and conversion. In this work, the same methodology was followed in order to assess

Table 1 – Performance parameters.

Performance parameters	
Raffinate purity (%)	$PUR = 100 \int_t^{t+N_c t^*} C_{R,C} dt / \left(\int_t^{t+N_c t^*} (C_{R,B} + C_{R,C} + C_{R,D}) dt \right)$
Extract purity (%)	$PUX = 100 \int_t^{t+N_c t^*} C_{X,D} dt / \left(\int_t^{t+N_c t^*} (C_{X,B} + C_{X,C} + C_{X,D}) dt \right)$
Conversion (%)	$X = 1 - \left(Q_X \int_t^{t+N_c t^*} C_{X,B} dt + Q_R \int_t^{t+N_c t^*} C_{R,B} dt \right) / (Q_F C_{F,B} N_c t^*)$
Productivity ($kg_C/(day\, L_{adsorbent})$)	$PR = Q_R \int_t^{t+N_c t^*} C_{R,C} dt / ((1-\varepsilon) V_c N_c t^*)$
Desorbent consumption (L_A/Kg_C)	$DC = N_c t^* (Q_D C_{D,A} + Q_F (C_{F,A} - v_A X C_{F,B})) / \left(Q_R \int_t^{t+N_c t^*} C_{R,C} dt \right)$

Table 2 – Characteristics of the columns for both SMBR and PermSMBR.

	SMBR	PermSMBR	Coupled PermSMBR	
			Fixed-bed column	Pervaporation module
Solid weight (A15)	47.6 g	47.6 g	47.6 g	–
Length of the bed (L)	23 cm	25.45 cm	23 cm	25.45 cm
Internal diameter (D_i)	2.6 cm	0.7 cm[a]	2.6 cm	0.7 cm[a]
Bed porosity (ε)	0.4	0.424	0.4	–
Bulk density (ρ_b)	390 kg/m^3	374 kg/m^3	390 kg/m^3	–
Number of membranes	–	13	–	13

[a] Membrane internal diameter.

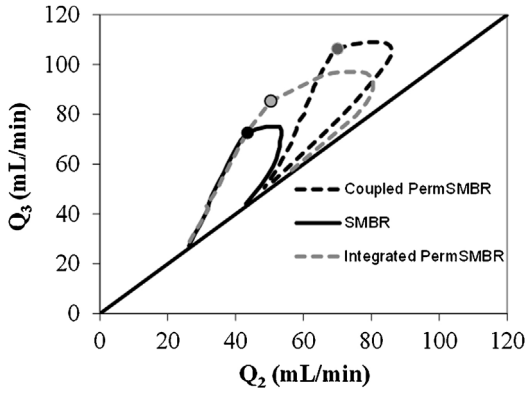

Fig. 4 – Reactive separation regions for the SMBR, PermSMBR and coupled PermSMBR for the following operating conditions: feed of 51% of acetaldehyde in n-butanol; configuration of 3 columns per section; temperature of 50 °C; t^*_{SMBR} = 3.1 min, $t^*_{PermSMBR}$ = 3.4 min, $t^*_{coupled\ PermSMBR}$ = 3.1 min, and desorbent and recycle flow rates of 105 and 21 mL/min, respectively. SMBR optimal operating point; integrated PermSMBR optimal operating point; coupled PermSMBR optimal operating point.

the performance of the coupled PermSMBR when compared with the performance of SMBR and integrated PermSMBR.

The reactive separation regions for 95% purity of extract and raffinate streams and for 95% conversion, for the coupled PermSMBR, the integrated PermSMBR and the SMBR, defined by the liquid flow rates at the beginning of section 2 and 3, because, along with the columns of each section, there will be flow rate fluctuations caused by adsorption/desorption and permeation (integrated and coupled PermSMBR) of the species, are shown in Fig. 4.

For the construction of these reactive separation regions, for each feed flow rate, the flow rate in section 2 was changed. The flow rate in section 3 was calculated from the mass balance in the feed node for each flow rate in section 2. For each set of flow rates in sections 2 and 3, the conversion and the purities of the extract and the raffinate were estimated and the values that satisfy the criteria of 95% were selected to build the reaction/separation regions. This procedure was repeated until the maximum value of feed flow rate that gives required product purities and conversion was achieved, which corresponds to the vertex of the reactive separation region (optimal operating point). Above that feed flow rate value the requirements cannot be fulfilled for any pair of flow rates in sections 2 and 3.

In all cases, n-butanol was used as desorbent and the operating conditions were as follows: feed of 51% of acetaldehyde in n-butanol; temperature of 50 °C; desorbent and recycle flow rates of 105 and 21 mL/min, respectively. For the SMBR the switching time considered was 3.1 min, while for the PermSMBR the switching time was set to 3.4 min in order to have the same velocities in sections 1 and 4 (Silva et al., 2010). For the coupled PermSMBR this equivalence is not straightforward and therefore, it was considered the same switching time as in the SMBR. Additionally, for the integrated and coupled PermSMBR, the permeate pressure was set at 5 mbar. The adopted configuration was 3–3–3–3 for SMBR and PermSMBR, and 3(3)–3(3)–3(3)–3(3) for the coupled PermSMBR that means 3 columns plus 3 membrane modules per section (the number of membrane modules is indicated between brackets).

As can be depicted from Fig. 4, the larger reactive separation region corresponds to the PermSMBR, as expected, since usually the integrated processes, at appropriate conditions for all the integrated steps, in this case suitable conditions for reaction and separation by adsorption and permeation, lead to the best results. However, at a first glance, what is surprising is that at the optimal operating points (vertex of the reactive separation regions), the coupled PermSMBR has a slight increased productivity (69.14 $kg_{DBE}/(L_{resin}\ day)$) and lower desorbent consumption (1.97 $L_{n\text{-}Butanol}/kg_{DBE}$) than the integrated PermSMBR (64.15 $kg_{DBE}/(L_{resin}\ day)$; 2.15 $L_{n\text{-}Butanol}/kg_{DBE}$). This can be justified by the fact that the integrated PermSMBR and the coupled PermSMBR are not being compared at the same conditions. As mentioned above, the SMBR switching time was 3.1 min, while the switching time of the PermSMBR was 3.4 min. These different values were set in order to have the same liquid and simulated solid velocities in sections 1 and 4 for both technologies. At the switching time, all the inlet and outlet streams of the SMBR and PermSMBR are switched one column ahead in the direction of the liquid in order to simulate the counter-current movement of the solid (see Figs. 1 and 2). The simulated solid velocity is then given by the length of the column divided by the switching time for both SMBR and integrated PermSMBR processes.

In the coupled PermSMBR, at the switching time, all the inlet and outlet streams are switched one column plus one membrane module ahead, also, in the direction of the liquid (see Fig. 3). And so, for the coupled PermSMBR the solid velocity cannot be calculated by the same way. The switching time should be corrected in order to compensate the residence time in the membrane modules to have the same solid velocity as in the previous technologies. However, this is not so simple, because the residence time in the membrane module is different in each section (due to the different flow rates). For instance in section 1, the residence time in the membrane module (13 membranes in parallel) is about 1 min, while in section 4 the residence time is equal to 6 min. Therefore, as an approximation, it was considered an average residence time in the membranes that is equal to about 2.06 min, which led to a switching time of 5.16 min for the coupled PermSMBR technology. The reactive separation regions for the coupled PermSMBR for a switching time of 3.1 min and of 5.16 min are shown in Fig. 5. As can be observed, the shape of the reactive separation region for the switching time of 3.1 min is completely different from that for a switching time of 5.16 min, which is mainly caused by the incomplete regeneration of the solid in section 1 when 3.1 min are considered. The

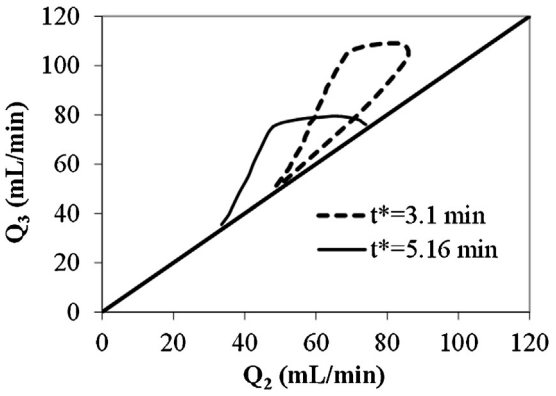

Fig. 5 – Coupled PermSMBR reactive separation regions at two different switching times: 3.1 min and 5.16 min.

Table 3 – Performance parameters at the optimal operating conditions.

	SMBR	PermSMBR	Coupled PermSMBR	
			$t^* = 3.1$ min	$t^* = 5.16$ min
PR ($kg_{DBE}\ L_{resin}^{-1}\ day^{-1}$)	53.15	64.15	69.14	48.52
DC ($L_{n\text{-}Butanol}/kg_{DBE}$)	2.69	2.15	1.97	3.00

Table 4 – SMBR performance parameters at the optimal operating conditions (for 95% purity and 95% conversion criteria) for different switching times.

t^* (min)	PR ($kg_{DBE}\ L_{resin}^{-1}\ day^{-1}$)	DC ($L_{n\text{-}Butanol}/kg_{DBE}$)
3.5	51.04	2.99
3.3	52.55	2.89
3.2	53.18	2.84
3.1	53.39	2.83
3.0	52.75	2.87
2.9	51.08	2.98

performance parameters at the optimal operating points (vertex of the reactive separation regions) are presented in Table 3 for the SMBR, the integrated and coupled PermSMBR. The coupled PermSMBR performance was strongly compromised with the increase of the switching time from 3.1 to 5.16 min, being even worse than the performance of the SMBR.

5.2.2. *Effect of the switching time*

In order to try to compare the SMBR, integrated PermSMBR and coupled PermSMBR in a fair way, it was determined the switching time that leads to the best performance for each one of the technologies. This was made by determining the optimal operating points, once again obeying to the criteria of 95% purity and conversion, for different switching times and keeping constant the following operating conditions: feed of 51% of acetaldehyde in n-butanol; configuration of 3–3–3–3; temperature of 50 °C; desorbent and recycle flow rates of 110 and 18 mL/min, respectively, and, for the PermSMBR and coupled PermSMBR, permeate pressure of 5 mbar.

Clearly, the performance of the PermSMBR (integrated or coupled) is better than the performance of the SMBR at the optimal switching time for the studied conditions (see Tables 4, 5 and 6). With regard to the PermSMBR, the integrated solution presents just a slight enhanced result (PR = 69.70 $kg_{DBE}\ L_{resin}^{-1}\ day^{-1}$; DC = 2.04 $L_{n\text{-}Butanol}/kg_{DBE}$; $t^* = 2.5$ min) when compared with the coupled one (PR = 69.42 $kg_{DBE}\ L_{resin}^{-1}\ day^{-1}$; DC = 2.07 $L_{n\text{-}Butanol}/kg_{DBE}$; $t^* = 3.0$ min). Nevertheless, as can be observed in Fig. 6, the integrated PermSMBR reactive separation region at optimal switching time is larger than the reactive separation region of the coupled process, which means that a more extensive range of operating conditions can be applied to fulfil the predefined requirements of purities and conversion. In both cases, for low feed flow rates, the reactive separation regions are narrower, due to the incomplete regeneration of the adsorbent (A15 resin) in section 1 when these switching time values are considered.

Table 5 – PermSMBR performance parameters at the optimal operating conditions (for 95% purity and 95% conversion criteria) for different switching times.

t^* (min)	PR ($kg_{DBE}\ L_{resin}^{-1}\ day^{-1}$)	DC ($L_{n\text{-}Butanol}/kg_{DBE}$)
3.5	63.34	2.31
3.3	65.08	2.23
3.0	67.28	2.14
2.8	68.42	2.09
2.7	68.89	2.07
2.6	69.39	2.05
2.5	69.70	2.04
2.4	69.24	2.05
2.3	69.22	2.05
2.1	64.89	2.21

Table 6 – Coupled PermSMBR performance parameters at the optimal operating conditions (for 95% purity and 95% conversion criteria) for different switching times.

t^* (min)	PR ($Kg_{DBE}\ L_{resin}^{-1}\ day^{-1}$)	DC ($L_{n\text{-}Butanol}/kg_{DBE}$)
3.5	65.64	2.23
3.3	67.42	2.15
3.1	68.81	2.09
3.0	69.42	2.07
2.9	69.33	2.06
2.8	68.68	2.08
2.7	66.50	2.16

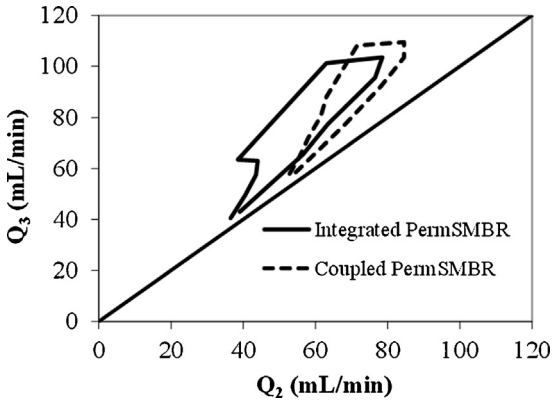

Fig. 6 – Reactive separation regions of the integrated and coupled PermSMBR at the optimal switching times (2.5 min – integrated PermSMBR; 3.0 min – coupled PermSMBR).

As stated in the Section 1, the implementation and maintenance of the coupled PermSMBR are easier tasks than in the integrated solution. Moreover, the coupled process has more degrees of freedom: the membranes and packed columns are independent, being possible to optimize each unit separately. Therefore, the assessment of the coupled PermSMBR technology is of value and it will be presented in the following section.

5.3. *Coupled PermSMBR*

5.3.1. *Effect of the number of membranes*

The effect of the number of membranes (in each module) was studied (Fig. 7 and Table 7), keeping the other operating conditions (feed of 51% of acetaldehyde in n-butanol; configuration of 3(3)–3(3)–3(3)–3(3); temperature of 50 °C; switching time of 3.1 min; permeate pressure of 5 mbar; desorbent and recycle flow rates of 105 and 21 mL/min, respectively).

Table 7 – Performance parameters at the optimal operating conditions (for 95% purity and 95% conversion criteria) for different membrane area.

Membrane number (area)	13 (87 dm^2)	6 (40 dm^2)	3 (20 dm^2)	0 (0 dm^2)[a]
PR ($kg_{DBE}\ L_{resin}^{-1}\ day^{-1}$)	69.14	62.06	57.83	53.15
DC ($L_{n\text{-}Butanol}/kg_{DBE}$)	1.97	2.24	2.43	2.69

[a] SMBR.

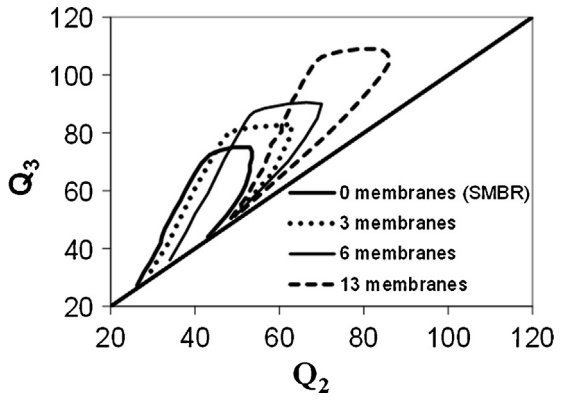

Fig. 7 – Coupled PermSMBR reactive separation regions for different number of membranes.

The improvement of the coupled PermSMBR productivity by increasing the number of membranes from 6 to 13 is not so significant. At the optimal operating points an increase of 11% on productivity and decrease of 12% on the desorbent consumption are noticed (Table 7). Besides, the 13 membranes reactive separation region is even smaller than the 6 membranes reactive separation region, which is due to the longer residence time on 13 membrane modules that implies: (i) a smaller liquid to solid velocity ratio leading to incomplete regeneration of resin in section 1 and (ii) higher mass transfer resistance in the membranes boundary layer that leads to lower water permeation rate. The performance parameters at the optimal operating points in absence of concentration polarization effects are presented in Table 8. These results, when compared with the ones presented in Table 7, prove that the concentration polarization is more significant for the higher membranes number as expected, but are not the only reason for the difference in the size of the reactive separation regions.

From this analysis, it can be concluded that the study of the effect of the number of membranes into the coupled

Table 8 – Performance parameters at the optimal operating conditions (for 95% purity and 95% conversion criteria) for different membrane area in absence of concentration polarization effects.

Membrane number (area)	13 (87 dm^2)	6 (40 dm^2)	3 (20 dm^2)
PR ($kg_{DBE}\ L_{resin}^{-1}\ day^{-1}$)	71.40	63.05	58.21
DC ($L_{n\text{-}Butanol}/kg_{DBE}$)	1.89	2.20	2.41

PermSMBR performance is not direct; changing the membranes number implies changing important conditions of the coupled PermSMBR operation. Probably, the best way is to find the operating conditions for each number of membranes that lead to the higher coupled PermSMBR performance.

5.3.2. *Coupled PermSMBR-3s*

As the integrated PermSMBR technology (Silva et al., 2010; Pereira et al., 2012), the coupled PermSMBR can be reduced from four to three sections, depending on the permeable compound, through the elimination of the extract or of the raffinate stream. In this case, the membranes are water selective and therefore, the coupled PermSMBR can be reduced to three sections (coupled PermSMBR-3s) by the elimination of the extract stream, which change the previous configuration 3(3)–3(3)–3(3)–3(3) to 6(6)–3(3)–3(3). In this configuration mode, the less adsorbed product (DBE) is still collected in the raffinate stream that is now located at the outlet of section 2, while the most adsorbed product (water) is removed just through the membranes (see Fig. 8). The coupled PermSMBR-3s was evaluated for the DBE synthesis; first it were considered the operating conditions that previously led to the highest productivity: feed of 51% of acetaldehyde in n-butanol; temperature of 50 °C; permeate pressure of 5 mbar, switching time of 3.0 min and recycle flow rates of 18 mL/min. In this case, for each feed flow rate the desorbent flow rate was changed in order to find the values that satisfy the 95% purity and

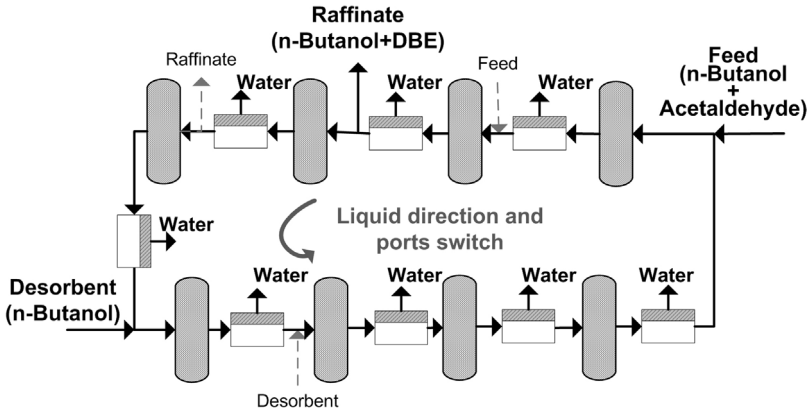

Fig. 8 – Schematic representation of a coupled PermSMBR unit for DBE synthesis with just 3 sections: section 1, between desorbent and feed nodes, comprising 4 columns and 4 membrane modules; section 2, between feed and raffinate nodes and section 3, between raffinate and desorbent nodes, comprising 2 columns and 2 membrane modules each.

conversion criteria. At 50 °C the water removal through the membranes was not enough to obtain DBE in the raffinate with 95% purity. Therefore, the temperature of the coupled PermSMBR-3s was increased to 70 °C. At this temperature, the highest productivity obtained (for 95% purity and conversion) is 73.44 $kg_{DBE}\,L_{resin}^{-1}\,day^{-1}$ with a desorbent consumption of 0.89 $L_{n\text{-}Butanol}/kg_{DBE}$. Compared with the coupled PermSMBR with 4 sections, the coupled PermSMBR-3s leads to more concentrated products (less 57% of n-butanol used as desorbent) and only one stream has to be treated (the raffinate). As consequence, the global costs associated to the downstream separation units are lower, which might compensate the temperature of operation increase from 50 to 70 °C. As for the integrated PermSMBR (previously evaluated) (Pereira et al., 2012), the coupled technology operated with just 3 sections seems to be the most attractive solution. Similar productivities are achieved using the integrated and the coupled PermSMBR-3s, but in the integrated solution the solvent savings are even more significant (integrated PermSMBR-3s: DC = 0.42 $L_{n\text{-}Butanol}/kg_{DBE}$).

A deeper study can be performed for the evaluation of the coupled PermSMBR considering the membranes arranged in series (instead of parallel). Such arrangement leads to the increase of the velocity improving the mass transfer in the boundary layer. Also one should optimize the membrane area (there are sections where the number of membranes could be reduced or even eliminated) and search for the best operating conditions considering the effect of flow rates in sections 1 and 4. However, the results obtained are enough to demonstrate the potential of this new PermSMBR set-up for the production of DBE and to motivate a deeper study in the future.

6. Conclusions

At the optimal operating points (for the studied conditions) the integrated and coupled PermSMBR have similar performance for the production of DBE. However, within the integrated set-up a more extensive range of operating conditions can be applied to fulfil the requirements of 95% purity and 95% acetaldehyde conversion. For both, integrated and coupled PermSMBR set-ups, the operation with just three sections (without extract stream), when compared with the operation with four sections, seems to be the best solution to efficiently produce DBE. Similar productivities are achieved using the integrated and the coupled PermSMBR-3s, but in the integrated solution the solvent savings are significantly lower (integrated PermSMBR-3s: DC = 0.42 $L_{n\text{-}Butanol}/kg_{DBE}$, coupled PermSMBR-3s: DC = 0.89 $L_{n\text{-}Butanol}/kg_{DBE}$).

These results together with the easiness maintenance of membranes and their higher mechanical and chemical stability (compared with the integrated PermSMBR) indicate that the coupled PermSMBR might be an attractive solution for the sustainable synthesis of oxygenated compounds that involve equilibrium limited reactions as is the case of DBE.

Acknowledgements

The research leading to these results has received funding from the European Union Seventh Framework Programme (FP7/2007-2013) under grant agreement n° 241718 Eurobioref.

Carla Pereira gratefully acknowledges financial support from Fundação para a Ciência e a Tecnologia, Postdoctoral Research Fellowship SFRH/BPD/71358/2010.

Appendix A.

A.1. Reaction equilibrium and kinetics

The reaction equilibrium constant (K_{eq}) was experimentally determined and is described by the Arrhenius equation (Graça et al., 2010b):

$$K_{eq} = 0.00959 \exp\left(\frac{1755.3}{T(K)}\right) \tag{A.1}$$

The reaction kinetics is described by a two-parameter kinetic law based on a Langmuir–Hinshelwood rate expression, using activity coefficients from the UNIFAC method (Graça et al., 2010b):

$$r = k_c \frac{a_A a_B - a_C a_D/(a_A K_{eq})}{\left(1 + K_{s,D} a_D\right)^2} \tag{A.2}$$

where:

$$k_c = 2.39 \times 10^9 \exp\left[\frac{-6200.9}{T(K)}\right] \left(\frac{mol}{g_{cat}\,\mathrm{min}}\right) \tag{A.3}$$

$$\text{and} \quad K_{S,D} = 2.25 \times 10^{-4} \exp\left[\frac{3303.1}{T(K)}\right] \tag{A.4}$$

A.2. Adsorption equilibrium

The adsorption data, obtained for A15, at 25 °C, by frontal chromatography experiments in a fixed-bed adsorber, is described by the multicomponent equilibrium adsorption Langmuir isotherm (Graça et al., 2010a):

$$\bar{q}_i = \frac{Q_{ads,i} K_i \bar{C}_{p,i}}{1 + \sum_{j=1}^{NC} K_j \bar{C}_{p,j}} \tag{A.5}$$

with the adsorption parameters presented in Table A.1.

Table A.1 – Multicomponent Langmuir isotherm parameters at 25 °C.

Component	Q_{ads} (mol/$L_{wet\,solid}$)	K (L/mol)
n-Butanol	8.5	7.5
Acetaldehyde	15.1	0.5
Water	44.9	12.1
DBE	5.8	0.4

In this work, the operating temperature is set at 50 °C and 70 °C, therefore, an approximation is made considering that adsorption parameters at these temperatures are the same as those at 25 °C. The validity of this approximation was checked in a previous work (Pereira et al., 2012).

A.3. Pervaporation data

The pervaporation process using two commercial hydrophilic silica membranes (from Pervatech) was evaluated for the DBE system (Pereira et al., 2012). In the absence of mass transfer limitations, the membranes performance was evaluated experimentally for binary (water and n-butanol) and quaternary mixtures (water, n-butanol, acetaldehyde and DBE), at different compositions and at two temperatures, 50 °C and 70 °C, measuring the total flux and

composition of the permeate. It was found that the permeances of water are $(4.43 \pm 0.66) \times 10^{-6}$ mol/(Pa s m^2) at 50 °C and $(3.93 \pm 0.94) \times 10^{-6}$ mol/(Pa s m^2) at 70 °C, the n-butanol permeances are $(9.84 \pm 2.21) \times 10^{-9}$ mol/(Pa s m^2) at 50 °C and $(6.48 \pm 2.07) \times 10^{-9}$ mol/(Pa s m^2) at 70 °C, the acetaldehyde flux is negligible with a permeance of $(7.93 \pm 4.24) \times 10^{-10}$ mol/(Pa s m^2) at 70 °C, and that DBE does not permeate through the membrane.

References

Boennhoff, K., Obenaus, F. 1,1-Diethoxyethane as diesel fuel. DE Patent 2 911, 1980.

Broughton, D.B., Gerhold, C.G. Continuous Sorption Process Employing Fixed Bed of Sorbent and Moving Inlets and Outlets. US Patent 2 985 589, 1961.

Glueckauf, E., 1955. Theory of chromatography. Trans. Faraday Soc. 51, 1540–1551.

Graça, N.S., Pais, L.S., Silva, V.M.T.M., Rodrigues, A.E., 2010a. Dynamic study of the synthesis of 1,1-dibutoxyethane in a fixed-bed adsorptive reactor. Sep. Sci. Technol. 46, 631–640.

Graça, N.S., Pais, L.S., Silva, V.M.T.M., Rodrigues, A.E., 2010b. Oxygenated biofuels from butanol for diesel blends: synthesis of the acetal 1,1-dibutoxyethane catalyzed by amberlyst-15 ion-exchange resin. Ind. Eng. Chem. Res. 49, 6763–6771.

Graça, N.S., Pais, L.S., Silva, V.M.T.M., Rodrigues, A.E., 2011. Analysis of the synthesis of 1,1-dibutoxyethane in a simulated moving-bed adsorptive reactor. Chem. Eng. Process.: Process Int. 50, 1214–1225.

Levenspiel, O., 1999. Chemical Reaction Engineering, third ed. John Wiley & Sons, New York.

Lévêque, M.A., 1928. Les lois de transmission de chaleur par convection. Ann. Mines 13, 201.

Pereira, C.S.M., Silva, V.M.T.M., Rodrigues, A.E., 2012. Green fuel production using the PermSMBR technology. Ind. Eng. Chem. Res. 51, 8928–8938.

Perkins, L.R., Geankoplis, C.J., 1969. Molecular diffusion in a ternary liquid system with the diffusing component dilute. Chem. Eng. Sci. 24, 1035–1042.

Rodrigues, A.E., Pereira, C.S.M., Santos, J.C., 2012. Chromatographic reactors. Chem. Eng. Technol. 35, 1171–1183.

Ruthven, D.M., 1984. Principles of Adsorption and Adsorption Processes. Wiley & Sons, New York.

Santacesaria, E., Morbidelli, M., Servida, A., Storti, G., Carra, S., 1982. Separation of xylenes on Y zeolites. 2. Breakthrough curves and their interpretation. Ind. Eng. Chem. Process Des. Dev. 21, 446–451.

Silva, V.M.T.M., Pereira, C.S.M., Rodrigues, A.E. Simulated Moving Bed Membrane Reactor, New Hybrid Separation Process and used thereof. PT Patent 104496; WO Patent 2010/116335, 2009.

Silva, V.M.T.M., Pereira, C.S.M., Rodrigues, A.E., 2010. PermSMBR—a new hybrid technology: application on green solvent and biofuel production. AlChE J. 57, 1840–1851.

Silva, V.M.T.M., Rodrigues, A.E., 2002. Dynamics of a fixed-bed adsorptive reactor for synthesis of diethylacetal. AIChE J. 48, 625–634.

Wijmans, J.G., Athayde, A.L., Daniels, R., Ly, J.H., Kamaruddin, H.D., Pinnau, I., 1996. The role of boundary layers in the removal of volatile organic compounds from water by pervaporation. J. Membr. Sci. 109, 135–146.